FIRST ATTEMPTS TO ACCOUNT FOR FLEXIBLE MODES IN ACT/FHS SYSTEM IDENTIFICATION

Susanne Seher-Weiß
German Aerospace Center (DLR), Institute of Flight Systems
Lilienthalplatz 7, D-38108 Braunschweig, Germany
susanne.seher-weiss@dlr.de

ABSTRACT

At the DLR Institute of Flight Systems mathematical models of the ACT/FHS (Active Control Technology/Flying Helicopter Simulator), an EC135 with a highly modified control system, are needed for control system development and simulation. So far, the models that have been derived by system identification account for rotor and engine dynamics. For comfort of ride investigations, and to improve the model quality for frequencies above 20 rad/s, the influence of flexible modes also has to be modeled. For the ACT/FHS the largest effect is the influence of vertical tail bending on pitch rate. The investigation started with a single-input/single-output system for pitch rate response to collective control inputs that was extended by one structural mode for tail flexibility. As this approach was successful, next an identified 17th order model of the ACT/FHS was also extended by one flexible mode. In this model, the structural mode was still dynamically decoupled from the 17th order model and its influence on pitch rate and longitudinal and vertical acceleration was described by influence factors in the output equations. Finally, a one-way coupled hybrid model was identified that extends the influence of the structural modes to other input/output combinations. Accounting for tail flexibility in this way extended the range of validity of the identified model up to the nominal rotor speed of 41 rad/s.

NOMENCLATURE

$\boldsymbol{A}$, $\boldsymbol{B}$	stability and control matrix
a_x, a_y, a_z	longitudinal, lateral, and vertical acceleration, m/s^2
C	structural mode coupling derivatives
L, M, N	moment derivatives
p, q, r	roll, pitch and yaw rates, rad/s
S	structural mode control derivatives
s	Laplace variable, 1/s
u, v, w	body-fixed velocity components, m/s
$\boldsymbol{u}$, $\boldsymbol{x}$, $\boldsymbol{x}$	input, state, and output vectors
X, Y, Z	force derivatives
δ_{lon}, δ_{lat}	longitudinal and lateral cyclic inputs, %
δ_{col}, δ_{ped}	collective and pedal inputs, %
Φ, Θ	roll and pitch angles, rad
H	structural mode influence coefficients
η_1, η_2	structural mode displacement and rate states
τ	time delay, s
ζ_{str}	structural mode damping
ω_{str}	structural mode frequency, rad/s

Subscripts

m	measured value
rb	rigid-body
str	structural mode(s)
$17ord$	17th order model

Acronyms

ACT/FHS	Active Control Technology / Flying Helicopter Simulator
ML	maximum likelihood

1. INTRODUCTION

To ensure satisfactory handling and ride qualities, increasingly higher crossover frequencies (frequencies, where the magnitude crosses the stationary response) are required in the flight control systems. Flight control law design is usually conducted using linear models that describe the rigid-body dynamics and - if required - also rotor and/or engine dynamics. As long as the structural modes remain well separated from the crossover frequency (by a factor of at least 10-15 [1]), notch filters are sufficient to avoid potential interaction with the structural modes. Otherwise, the flexible modes have to be accounted for in the models used for control system design.

In ref. [2] it was shown that structural modes with frequencies below the rotor frequency have a strong impact on ride quality. The modeling of flexible modes is thus also important for comfort of ride investigations.

Accounting for flexible modes in system identification has been performed for fixed wing applications such as large flexible aircraft [3] or sailplanes [4]. Flexible modes were accounted for in the control system development for a large helicopter in ref. [5]. However, in this work, models for the flexible modes were not identified from flight test data but determined from shake tests using finite element software.

The general derivation of the equations of motion for coupled rigid-body/structural systems is described in ref. [6]. A good overview over different modeling approaches to account for flexible modes in system identification can be found in ref. [7].

The ACT/FHS (Active Control Technology / Flying Helicopter Simulator, see Fig. 1) is the main testbed for rotorcraft research at the German Aerospace Center (DLR) [8–10]. It is a highly modified Eurocopter EC135, a light twin-engine helicopter with a bearingless main rotor and a fenestron. The mechanical controls of the ACT/FHS have been replaced by a full-authority fly-by-wire/fly-by-light control system that allows applying control inputs generated by an experimental system in flight. Thus, the dynamics of the ACT/FHS are not comparable to data from a production EC135 rotorcraft.

Figure 1: DLR research helicopter ACT/FHS

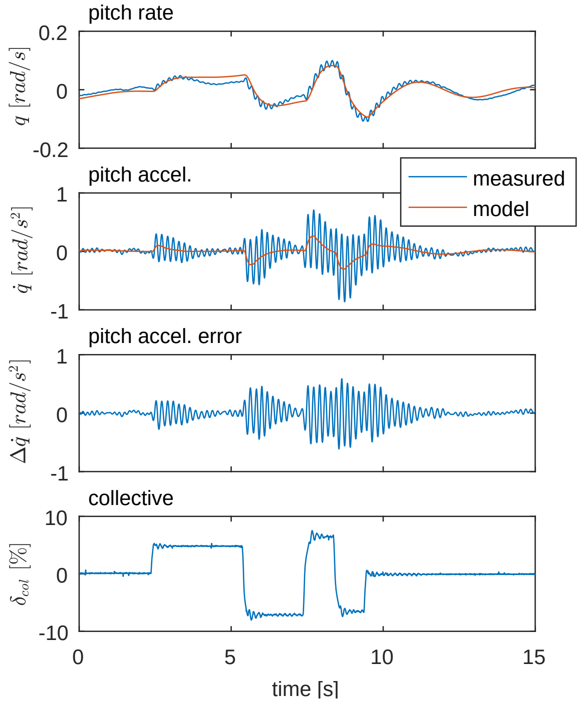

Figure 2: Remaining error in pitch axis for collective inputs (17th order model)

The crossover frequencies of the ACT/FHS control system are 3 rad/s for the pitch and 5 rad/s for the roll axis. As the models that are used to develop the control laws should ideally be accurate from one decade below to one decade above it ($\pm$ half a decade is usually sufficient), models are sought that cover the frequency range of at least 0.5-30 rad/s.

Investigations for the Bo105 [11] and shake tests from a production EC 135 indicated that the structural mode with the lowest frequency is the vertical tail bending with a frequency in the order of 35 rad/s and thus very close to the desired range of validity for the identified models. Compared to a production EC 135, the ACT/FHS has a heavier tail due to additional instrumentation. Therefore, monitoring of tail bending is mandatory when flying the ACT/FHS in experimental mode and the aircraft is thus equipped with strain gauges at the tail root.

System identification of the ACT/FHS yields the necessary models for the model-based control and in-flight simulation research activities at DLR. The most recently identified models of the ACT/FHS are of 17th order and account for the rotor degrees of freedom (flapping, inflow and regressive lead-lag) and contain a dynamic engine model [12].

Looking at the remaining error dynamics of these models, it can be seen that the error in pitch acceleration for collective inputs as shown in Fig. 2 for a 3211-multistep input maneuver is a pure damped oscillation. Comparison with strain gauge measurements indicated that this unmodeled oscillation is caused by vertical tail boom bending. (The slight oscillation on the control input is caused by control system feedback.)

The excitation of structural modes by the control inputs is normally suppressed by accordingly designed notch filters. At the time when the notch filters were designed for the ACT/FHS, excitation of the tail vertical mode had not yet been experienced for collective inputs. The corresponding frequency was therefore only accounted for in the notch filters for the cyclic and not the collective control input. As it is difficult to properly identify a structural mode if the corresponding frequency is suppressed by a notch filter, the off-axis response of pitch rate due to collective input was used as the basis for the current investigations.

The ACT/FHS is equipped with specialized flight test sensors, such as a high accuracy INS, a noseboom and two differential GPS receivers. But, except for strain gauges at the tail, the ACT/FHS is not equipped with dedicated sensors to measure structural deformations. As matching the strain gauge signals was not deemed necessary, is was tried to use the same instrumentation as utilized in the rigid-body/rotor/engine modeling efforts also for the derivation of models including flexible modes.

This paper uses ACT/FHS flight test data for the 60 knots forward flight case to investigate modeling elastic effects. First, the single-input/single-output (SISO) system of pitch rate due to collective control input will be augmented by one structural mode to account for tail flexibility.

The results from this modeling step will then be used as a starting point to extend a 17th order model of the ACT/FHS by one flexible mode. In this multiple-input/multiple-output (MIMO) model, the structural dynamics are still dynamically decoupled from the rigid-body/rotor/engine dynamics and only accounted for by influence factors in the output equations. Finally, a one-way coupled hybrid model will be derived and its results will be shown.

2. SINGLE-INPUT/SINGLE-OUTPUT MODELING

A full aeroelastic modeling of a flexible vehicle leads to partial differential equations as not only the motion of the center of gravity (CG) but also the movement of different mass points with respect to the CG have to be described. A modal analysis of such a vehicle leads to a mean-axis system and all structural deformations can then be described with respect to this axis system. The deformations are described as structural modes (eigenmodes) with corresponding eigenfrequency and damping. The modal synthesis then leads to a separation of variables, generating a differential equation for the rigid body (zero-th eigenmode, corresponding to a frequency of zero), and a set of second order equations for the generalized coordinates, describing the amplitudes of the modal deflections.

As the influence of tail flexibility for the ACT/FHS is most pronounced in pitch rate due to collective control inputs, the transfer function q/δ_{col} was first investigated as a SISO system. A 1st order response was assumed for the rigid-body part of q/δ_{col}. Following the approach of Tischler (see chapter 16.4 of [7]), one second order system for the tail flexibility mode was then added in a partial fraction expansion.

$$\frac{q}{\delta_{col}} = \frac{M_{\delta_{col}}}{s - M_q} + \frac{S_{\delta_{col}} s}{s^2 + 2\zeta_{str}\omega_{str} s + \omega_{str}^2} \tag{1}$$

The first term on the right-hand side is the rigid-body pitch response and the second term is the vertical tail bending structural mode with a frequency of ω_{str} and a damping of ζ_{str}. The collective control input excites both the rigid-body and structural modes via the control derivatives $M_{\delta_{col}}$ and $S_{\delta_{col}}$.

For identification, the partial fraction model of (1) was augmented by a time delay to account for unmodeled rotor dynamics and then implemented with the state equatiions

$$\begin{aligned}\begin{pmatrix}\dot{q}_{rb}\\ \dot{\eta}_1\\ \dot{\eta}_2\end{pmatrix} &= \begin{bmatrix} M_q & 0 & 0\\ 0 & 0 & 1\\ 0 & -\omega_{str}^2 & -2\zeta_{str}\omega_{str}\end{bmatrix}\begin{pmatrix} q_{rb}\\ \eta_1\\ \eta_2\end{pmatrix}\\ &+ \begin{bmatrix} M_{\delta_{col}}\\ 0\\ S_{\delta_{col}}\end{bmatrix}\delta_{col}(t - \tau_{\delta_{col}})\end{aligned} \tag{2}$$

Here, q_{rb} denotes the rigid-body contribution to the overall pitch rate. η_1 and η_2 are the modal displacement and

Parameter	Value	CR-Bound [%]
$M_{\delta_{col}}$	0.0107	11.58
M_q	-3.0	–
$\tau_{\delta_{col}}$	0.0419	3.63
$S_{\delta_{col}}$	-0.0778	4.97
ζ_{str}	0.0369	12.84
ω_{str}	34.1	0.47

Table 1: Identified parameters of the SISO model

modal rate (velocity) states of the structural mode. The overall pitch rate q is the sum of the rigid-body and structural contributions

$$q = \begin{bmatrix}1 & 0 & 1\end{bmatrix}\begin{pmatrix} q_{rb}\\ \eta_1\\ \eta_2\end{pmatrix} \tag{3}$$

Identification of the system from eqs. (2) and (3) was performed using the frequency response method [7, 13]. The frequency response data for q/δ_{col} was approximated over the frequency range of 10-40 rad/s. The corresponding identification results are listed in Tab. 1. The derivative M_q had to be fixed at the value identified from a 6-DoF model without flexible modes, because it could not accurately be identified from this cross-axis response. The frequency of the vertical tail bending mode is identified as 34.1 rad/s with a very low uncertainty level (Cramer-Rao bound).

It can be seen from Fig. 3 that the rise in amplitude and drop in phase at the higher frequencies is described sufficiently well by adding the structural tail mode in this way.

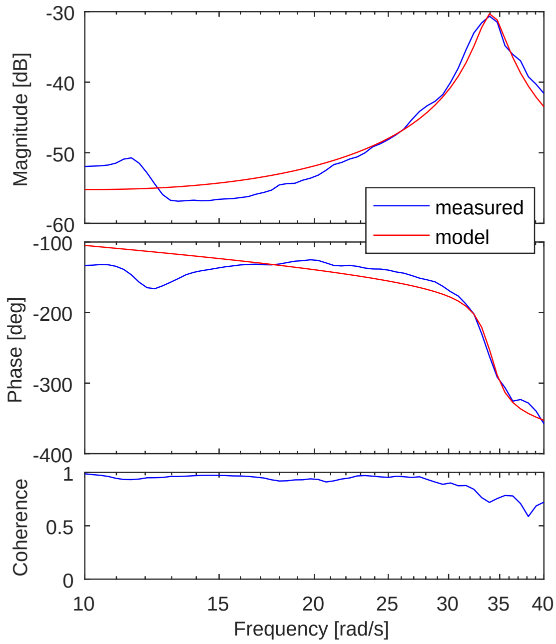

Figure 3: Frequency domain match of the SISO model for q/δ_{col} with added structural mode

Fig. 4 illustrates the corresponding match in the time domain for the same 3211-multistep input maneuver and with the same scaling as in Fig. 2. The oscillation in pitch acceleration $\dot{q}$ is now modeled correctly and the remaining error therefore drastically reduced compared to the model without structural modes. As this is only a SISO model, the overall match in pitch rate is of course not as good as for the fully coupled 17th order model used in Fig. 2.

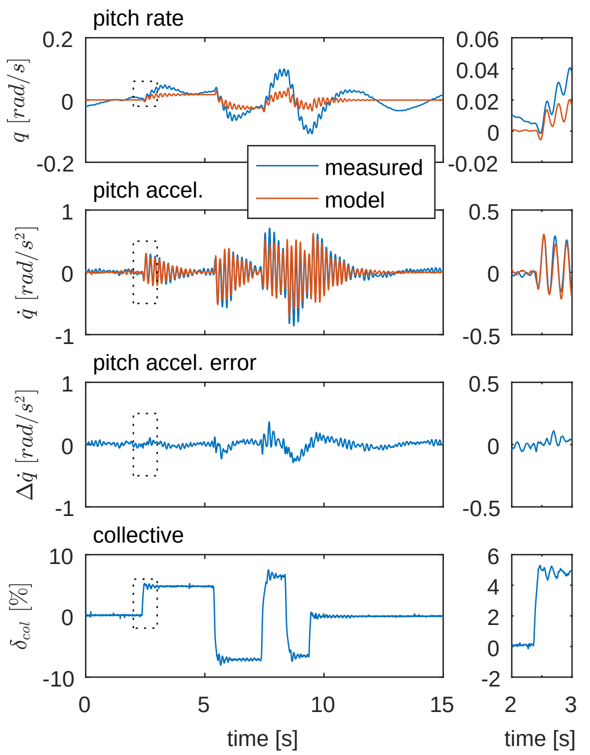

Figure 4: Time domain match of the SISO model for q/δ_{col} with added structural mode

Writing the resulting identified transfer function from eq. (1) in pole/zero formulation yields

$$\frac{q}{\delta_{col}} = -0.067\frac{(15.3)(-12.2)}{(3.00)[0.0369, 34.1]} \tag{4}$$

where $(1/T)$ is the shorthand notation for $(s + 1/T)$ and $[\zeta, \omega]$ is short for $s^2 + 2\zeta\omega s + \omega^2$. The transfer function has a zero in the right-hand plane which causes an initial response in the opposite direction to the control input as can be seen in the zoomed-in plots on the right side of Fig. 4.

Fig. 5 shows a root-locus plot of the transfer function from eq. (4) for varying pitch rate gain K_q. It can be seen that an increasing pitch rate feedback gain on collective would destabilize the tail structural mode.

It is important to note that there is no dynamic coupling between the rigid-body and structural states in eq. (2). Nevertheless, this assumption leads to a good match and provides a considerable extension in the frequency range of

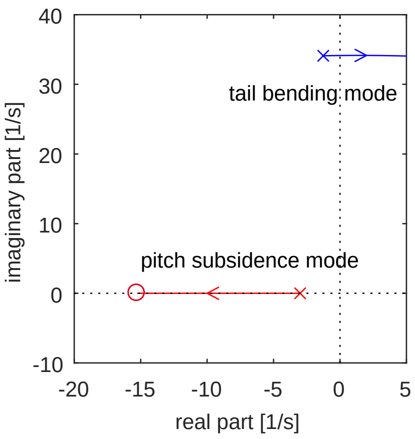

Figure 5: Root locus for pitch rate gain on collective

applicability of the identified extended model as compared to a rigid-body model structure. Another important observation is that the identification of this simple extended model is based solely on the fuselage angular response sensors and does not require additional flight-test measurements of the structural response.

3. GENERAL MIMO MODEL STRUCTURE

Assuming that the elastic displacements are small compared to the rigid-body motion, the dynamics of the flexible modes can be written with respect to a body-fixed mean axis system, a formulation commonly used in flight dynamics and control literature [1]. A consequence of this mean-axis formulation is that all coupling between the structural and rigid-body systems is via the aerodynamic forces and moments and there is no inertial coupling introduced into the mass matrix. The dynamics of the structural modes in normal coordinates can then be appended to the rigid-body equations of motion as mutually uncoupled sets of second-order differential equations.

In general, this means that the matrices of the coupled rigid-body/structural modes state equations can be partitioned as [7]

$$\boldsymbol{A} = \left[\begin{array}{c|c} \text{Rigid-Body Stability Derivatives} & \text{Aeroelastic Coupling Terms} \\ \hline \text{Rigid-Body Coupling Terms} & \text{Structural Flexibility Modes} \end{array}\right] \tag{5}$$

and

$$\boldsymbol{B} = \left[\begin{array}{c} \text{Rigid-Body Control Derivatives} \\ \hline \text{Structural Mode Control Derivatives} \end{array}\right] \tag{6}$$

and the state vector is also partitioned into rigid-body and structural components as

$$\boldsymbol{x} = \left[\begin{array}{c} \boldsymbol{x}_{rb} \\ \hline \boldsymbol{x}_{str} \end{array} \right] \tag{7}$$

The rigid-body states $\boldsymbol{x}_{rb}$ correspond to the motion of the fuselage reference axes. The structural state vector $\boldsymbol{x}_{str}$ consists of the generalized displacement state $\eta_{j,1}$ and rate (velocity) state $\eta_{j,2}$, for each structural mode j to be considered. They correspond to the state variables η_1 and η_2 in the simple SISO system from eq. (2). The number of structural modes to be included depends on the frequency range of interest.

Each sensor at a local position "a" measures the sum of the rigid-body motion of the fuselage reference axes and the elastic motion at location "a"

$$y_a = y_{rb} + y_{str} \tag{8}$$

For example, the pitch rate sensor at local position "a" measures contributions from both the rigid-body pitch rate q and local elastic rates $\eta_{j,2}$

$$q_a = q + H_{q_a,1}\eta_{1,2} + H_{q_a,2}\eta_{2,2} + \dots \tag{9}$$

where $H_{q_a,1}$, $H_{q_a,2}$, $\dots$ are the influence coefficients for $\eta_{1,2}$, $\eta_{2,2}$, $\dots$ at location "a." These influence coefficients convert the modal states to physical variables.

Similarly, a vertical accelerometer at local position "a" measures the sum of the rigid-body response and the local elastic contributions, but now, the elastic contributions are proportional to the modal accelerations $\dot{\eta}_{1,2}$, $\dot{\eta}_{2,2}$, $\dots$. Finally, the angular sensors measure the sum of the rigid-body response and elastic contributions that are proportional to the modal displacements $\eta_{1,1}$, $\eta_{2,1}$, $\dots$.

A fully coupled model as in eq. (5) can only be identified when additional measurements like strain gauges and accelerometers at different positions throughout the flexible vehicle are available. Of course, care has to be taken, that the sensors are not placed at a modal node. In ref. [4] such a fully coupled model was identified from flight test data of a flexible sailplane. In that project, besides an inertial measurement unit near the center of gravity, the instrumentation included three tri-axis accelerometers on each wing and two at the bottom and top of the vertical tail. Furthermore, one strain gauge on each wing, one on the center between the wings and one on the fuselage complemented the instrumentation.

Without such extra instrumentation, simplifications have to be made to arrive at a model structure where all model parameters are uncorrelated and identifiable.

3.1. Decoupled Model

Dropping both the rigid-body and the aeroelastic coupling terms in eq. (5) leads to state equations where the rigid-body and structural modes are dynamically decoupled. This is the MIMO extension of a simple SISO system like the one in eq. (2). The influence of the modal states on the output variables in such a dynamically decoupled system is solely described by influence coefficients H_{ij} in the measurement equations eq. (8).

In the ACT/FHS case, the state equations of the 17th order model from [12] were extended by one modal state for the tail flexibility, resulting in the following stability and control matrices

$$\boldsymbol{A} = \begin{bmatrix} \boldsymbol{A}_{17ord} & \boldsymbol{0}_{17,2} \\ \boldsymbol{0}_{2,17} & \begin{bmatrix} 0 & 1 \\ -\omega_{str}^2 & -2\zeta_{str}\omega_{str} \end{bmatrix} \end{bmatrix} \tag{10}$$

$$\boldsymbol{B} = \begin{bmatrix} \boldsymbol{B}_{17ord} \\ \begin{bmatrix} 0 & 0 & 0 & 0 \\ 0 & 0 & 0 & S_{\delta_{col}} \end{bmatrix} \end{bmatrix} \tag{11}$$

Here, $\boldsymbol{A}_{17ord}$ and $\boldsymbol{B}_{17ord}$ denote the stability and control matrices of the 17th order model corresponding to control inputs $\boldsymbol{u}^T = (\delta_{lon}, \delta_{lat}, \delta_{ped}, \delta_{col})$ and correspond to the rigid-body stability and control derivatives from eqs. (5) and (6). $\boldsymbol{0}_{n,m}$ denotes a n-by-m matrix of zeros

Denoting the modal displacement and rate states with η_1 and η_2 as in eq. (2), the output equations for $\dot{q}$, q and Θ as well as for a_x, a_z and u, w were extended by the influence of the vertical tail elastic mode states.

$$\begin{aligned} \Theta &= \Theta_{rb} + H_q\eta_1 \\ q &= q_{rb} + H_q\eta_2 \\ \dot{q} &= \dot{q}_{rb} + H_q\dot{\eta}_2 \\ u &= u_{rb} + H_u\eta_2 \\ a_x &= a_{x,rb} + H_u\dot{\eta}_2 \\ w &= w_{rb} + H_w\eta_2 \\ a_z &= a_{z,rb} + H_w\dot{\eta}_2 \end{aligned} \tag{12}$$

In these equations, variables with the index rb denote the output of the 17th order model without the structural influences and thus correspond to $\boldsymbol{y}_{rb}$ in eq. (8). As mentioned above, the elastic contribution on the pitch angle Θ is proportional to the modal displacement η_1 and the elastic contribution on the pitch rate q is proportional to the modal rate η_2. Consequently, the elastic contribution on the pitch acceleration $\dot{q}$ must be proportional to the modal acceleration $\dot{\eta}_2$. Because the elastic contribution on the linear accelerations a_x, a_z are proportional to the modal acceleration $\dot{\eta}_2$, the elastic contribution on the speed components u, w must be proportional to the modal rate η_2.

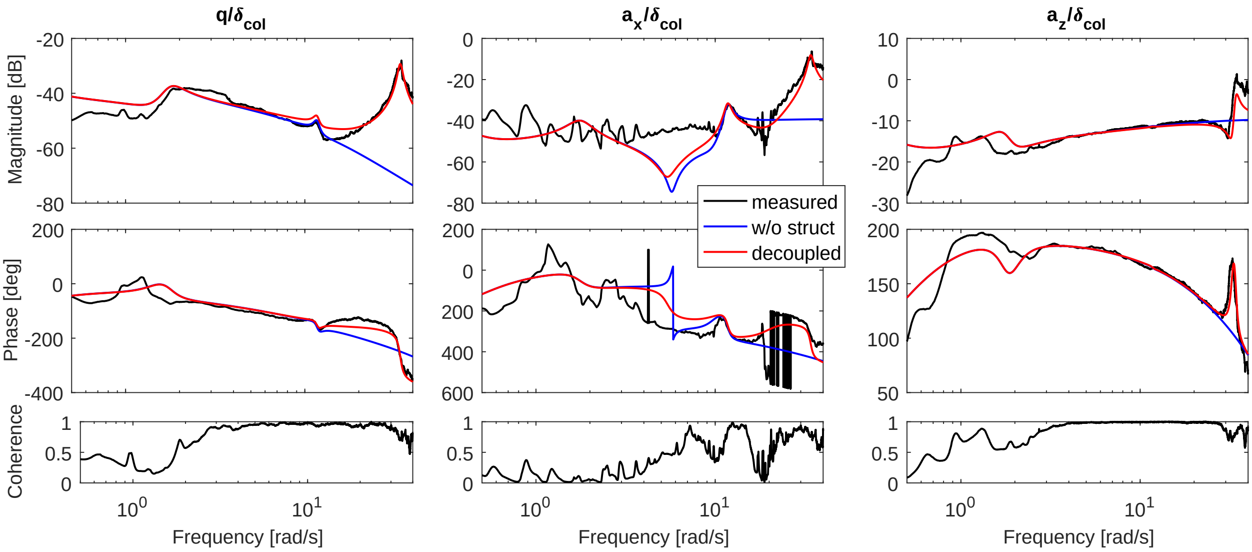

Figure 6: Frequency domain match of the MIMO model with decoupled structural mode

Parameter	Value	CR-Bound [%]
ζ_{str}	0.0309	3.98
ω_{str}	34.1	0.10
S_{str}	1.0	–
H_q	-0.0716	2.25
H_u	0.0240	6.14
H_w	-0.0290	7.71

Table 2: Identified modal parameters of the decoupled MIMO model

As the measurements of both q and $\dot{q}$ come from the same sensor package, they share a common influence coefficient H_q. Because of $\dot{\Theta} \approx q$, the pitch angle also shares the same influence coefficient. Similarly, both u and a_x share the influence coefficient H_u and the same is valid for w, a_z and the coefficient H_w.

For the identification of the flexible mode, the parameters of the 17th order model were kept fixed and only the parameters of the structural modes were estimated. As the control derivative $S_{\delta_{col}}$ and the influence factors H_q, H_u, and H_w are not independent, one of the parameters had to be fixed and thus the normalization $S_{\delta_{col}} = 1$ was chosen.

The identification was performed with the maximum likelihood (ML) method in the frequency domain [13] and a frequency range of 10-40 rad/s was used as the frequency range of 0.5-10 rad/s is already well covered by the 17th order model whose parameters remain unchanged. The values of the identified modal parameters and the corresponding Cramer-Rao bounds are listed in Tab. 2. It can be seen that the frequency and damping of the structural mode as well as the influence coefficients can be identified with small uncertainty.

Fig. 6 shows the resulting match in the transfer functions from collective control input to pitch rate and longitudinal and lateral acceleration in comparison to the 17th order model without added flexible mode. It can be seen, that by including the influence of tail flexibility, the match in amplitude and phase for q/δ_{col} is clearly improved in the high frequency range. Unlike for the SISO model from the previous section, the influence of tail flexibility is now also modeled in the transfer functions for a_x/δ_{col} and a_z/δ_{col}.

3.2. Hybrid Model

The generalized MIMO flight dynamics model from eqs. (5) and (6) includes full two-way dynamic coupling between the rigid-body and elastic states. This yields a complex identification model structure with many associated identification parameters and considerable parameter correlation and is thus not well suited to identification from flight test data.

In many applications, although the coupling of the rigid-body dynamics into the elastic states (rigid-body coupling) must be included for satisfactory modeling accuracy, the dynamic coupling of the elastic states into the rigid body equations of motion (aeroelastic coupling) can be assumed to be quasi-steady.

According to ref. [7], a prerequisite for this simplification is that the highest rigid-body mode and the lowest structural mode are separated by at least a factor of five. If this condition is fulfilled, the effect of structural bending on the rigid-body dynamics can be absorbed as correction increments, or flex factors, into the rigid-body quasi-steady stability and control derivatives. If only the most significant terms in the dynamic coupling of the rigid-body dynamics into the elastic states are retained, this leads to a so-called hybrid model structure [7].

Parameter	Value	CR-Bound [%]
ζ_{str}	0.0325	4.59
ω_{str}	33.7	0.14
C_u	0	–
C_w	26.0	5.91
C_q	-196	6.98
H_q	-0.0652	2.80
H_u	0.0188	5.89
H_w	-0.0290	–

Table 3: Identified modal parameters of the hybrid MIMO model

For the ACT/FHS, the rigid-body modes of the identified 17th model are (-0.012) for the spiral, $[-0.269, 0.211]$ for the phugoid, (-0.339) for the pitch subsidence mode and $[0.161, 1.78]$ for the dutch roll. Thus the separation by a factor of at least five with respect to the structural mode at 34 rad/s is given and the prerequisite for the application of the hybrid model structure therefore is fulfilled.

The one-way coupled equations for the hybrid model of the ACT/FHS were built with

$$\boldsymbol{A} = \begin{bmatrix} \boldsymbol{A}_{17ord} & \boldsymbol{0}_{17,2} \\ \boldsymbol{A}_{coup} & \begin{bmatrix} 0 & 1 \\ -\omega_{str}^2 & -2\zeta_{str}\omega_{str} \end{bmatrix} \end{bmatrix} \tag{13}$$

For the coupling matrix $\boldsymbol{A}_{coup}$ it was assumed that only the longitudinal states u, w, and q have an influence on the vertical tail elastic mode. As the first six states of the 17th order model are $\boldsymbol{x}^T = (u, v, w, p, q, r)$, this leads to

$$\boldsymbol{A}_{coup} = \begin{bmatrix} \begin{bmatrix} 0 & 0 & 0 & 0 & 0 & 0 \\ C_u & 0 & C_w & 0 & C_q & 0 \end{bmatrix} & \boldsymbol{0}_{2,11} \end{bmatrix} \tag{14}$$

The control matrix $\boldsymbol{B}$ is the same as for the decoupled model (see eq. (11)) and the output equations are also unchanged from eq. (12) for the decoupled model.

Identification was again performed with the ML method in the frequency domain. As the effect of the structural modes on the states of the 17th order model has to be modeled through increments on the stability and control derivatives, these parameters now had to be estimated. Therefore, the frequency range for the identification was extended to 0.5-40 rad/s. The model parameters pertaining to the regressive lead-lag and to the engine model [12] were kept fixed.

Tab. 3 lists the identified modal parameters. Coupling of the longitudinal velocity u into the states for vertical tail flexibility was not significant and the corresponding parameter C_u was therefore dropped from the identification. As the parameter H_w was not identifiable with the hybrid model, it was fixed at the value previously identified with the decoupled model. It can be seen that the identified values for the frequency and damping of the tail flexible mode are almost identical to those from the decoupled model (see Tab. 2). The influence coefficients H_q and H_u are also similar.

Par.	17th ord.	hybrid	CR-Bnd [%]	flex fact.
X_u	-0.0188	-0.0173	8.20	0.92
X_w	0.0257	0.0224	5.01	0.87
Y_v	-0.162	-0.163	1.14	1.01
Z_w	-0.695	-0.687	0.96	0.99
Z_p	0.658	0.793	10.30	1.21
L_v	-0.174	-0.177	1.09	1.02
L_w	0.110	0.107	2.34	0.97
L_r	-0.857	-0.993	4.17	1.16
M_v	0.0295	0.0289	2.21	0.98
M_w	0.0263	0.0266	2.98	1.01
N_u	-0.0124	-0.0114	5.81	0.92
N_v	0.0359	0.0349	1.82	0.97
N_p	-0.407	-0.422	1.90	1.04
N_r	-0.813	-0.849	1.59	1.04
$X_{\delta_{ped}}$	0.00293	0.00298	6.13	1.01
$Y_{\delta_{ped}}$	-0.0165	-0.0167	2.94	1.01
$Z_{\delta_{lon}}$	-0.0910	-0.0978	2.62	1.07
$M_{\delta_{ped}}$	0.00298	0.00293	4.80	0.98
$N_{\delta_{ped}}$	0.0231	-0.0234	0.76	1.01
L_b	-80.3	-75.6	0.97	0.94
M_a	-30.2	-27.3	1.37	0.90
τ_f	0.0696	0.0779	1.20	1.12
A_b	0.353	0.383	2.30	1.08
B_a	-0.325	0.345	4.43	1.06
$A_{\delta_{lon}}$	-0.00196	-0.00224	1.18	1.14
$A_{\delta_{lat}}$	0.00023	0.00026	3.67	1.14
$A_{\delta_{col}}$	-0.00079	-0.00088	1.35	1.12
$B_{\delta_{lon}}$	-0.00025	-0.00031	7.49	1.26
$B_{\delta_{lat}}$	-0.00227	-0.00249	1.16	1.10
$B_{\delta_{col}}$	-0.00053	-0.00061	2.30	1.14

Table 4: Identified quasi-static parameters and resulting flex factors

The identified values of the quasi-static parameters are listed in Tab. 4 (for a description of the model structure refer to [12]). The table gives the values of the 17th order model, those of the hybrid model including the Cramer-Rao bounds and the resulting flex factors (= hybrid model values divided by the corresponding value from 17th order model). Most flex factors are approximately one, especially if the uncertainty of the identified parameters as indicated by the Cramer-Rao bounds is taken into account. Nevertheless, there is a tendency towards reduced damping parameters (X_u, L_b, M_a) and increased control effectiveness ($A_{\delta_{lon}}$, $A_{\delta_{lat}}$, $B_{\delta_{lon}}$, $B_{\delta_{lat}}$) for the hybrid model.

Fig. 7 compares the match of the 17th order model without flexible modes, the decoupled model from the previous subsection and the hybrid model. It can be seen that by introducing the one-way coupling between the rigid-body and

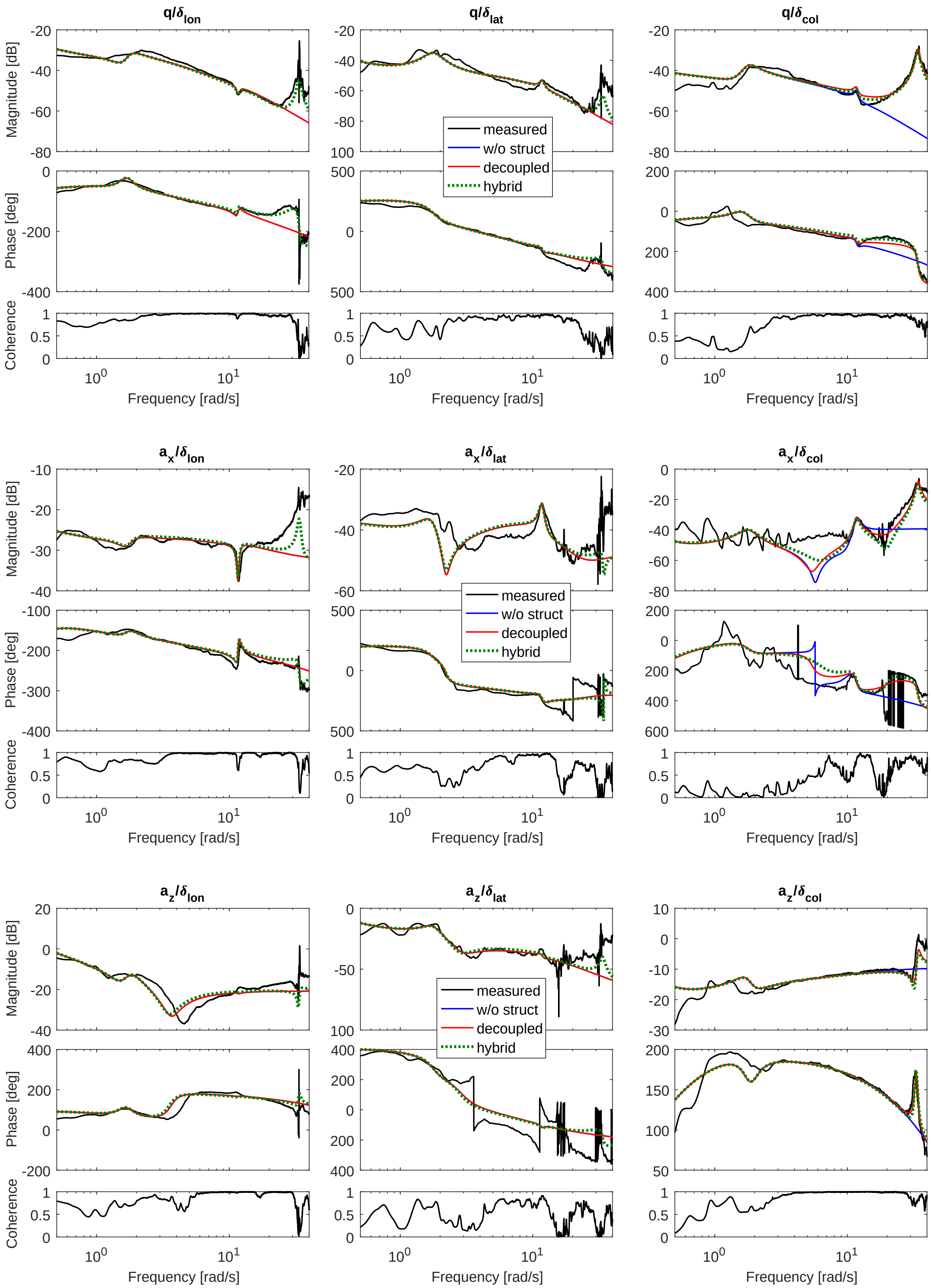

Figure 7: Frequency domain match of the hybrid MIMO model

the modal states, the match in q/δ_{col} is improved even further. In addition, the influence of the structural mode is now extended to the cyclic control inputs δ_{lon} and δ_{lat}.

4. SUMMARY AND OUTLOOK

High-bandwidth control systems with their high crossover frequencies need models that are accurate up to high frequencies and thus have to account not only for rotor degrees of freedom but also for structural modes. In the case of the ACT/FHS helicopter, the influence of tail flexibility mainly on pitch rate had to be accounted for.

The investigations led to the following conclusions:

- Extending the SISO transfer function from collective control input to pitch rate by one structural mode leads to a sufficiently well approximation in the high frequency region.
- Extending a previously identified 17th order model by one flexible mode, where the rigid-body/rotor/engine and the structural state equations are decoupled, allows to describe the influence of tail flexibility on pitch rate as well as longitudinal and vertical accelerations for collective control inputs.
- Adding a one-way coupling from the longitudinal rigid-body states (u, w,q) to the structural states allows to model the influence of tail flexibility also for several other input/output combinations

Overall, accounting for flexible modes in this way extended the frequency range of applicability of the identified model up to the rotor frequency (40 rad/s).

So far, only data for the 60 knots forward flight case were investigated. Next, the presented modeling approach will be applied to data from the whole flight envelope from hover up to 120 knots forward flight. Further investigations are planned to model the influence of structural modes also on the lateral-directional motion.

COPYRIGHT STATEMENT

REFERENCES

[1] David K. Schmidt. *Modern Flight Dynamics*. McGraw-Hill, New York, 2010.

[2] Tobias Rath and Walter Fichter. A closer look at the impact of helicopter vibrations on ride quality. In *AHS 73rd Annual Forum*, Fort Worth, TX, May 2017.

[3] Colin R. Theodore, Christina M. Ivler, Mark B. Tischler, Edmund J. Field, Randall L. Neville, and Heather P. Ross. System identification of large flexible transport aircraft. In *AIAA Atmospheric Flight Mechanics Conference and Exhibit*, Honolulu, HI, August 2008. AIAA 2008-6894.

[4] Bruno Giordano de Olivera Silva and Wulf Mönnich. System identification of flexible aircraft in time domain. In *AIAA Atmospheric Flight Mechanics Conference and Exhibit*, Minneapolis, MN, August 2012. AIAA 2012-4412.

[5] Vineet Sahasrabudhe, Alexander Faynberg, Maksym Pozdin, Rendy Cheng, Mark Tischler, Al Stumm, and Mike Lavin. Balancing CH-53K handling qualities and stability margin requirements in the presence of heavy external loads. In *AHS 63rd Annual Forum*, Virginia Beach, VA, May 2007.

[6] Martin R. Waszak and David K. Schmidt. Flight dynamics of aeroelastic vehicles. *Journal of Aircraft*, 6(25):563–571, 1988.

[7] Mark B. Tischler and Robert K. Remple. *Aircraft and Rotorcraft System Identification: Engineering Methods with Flight-Test Examples*. American Institute of Aeronautics and Astronautics, Inc., Reston, VA, 2nd edition, 2012. chapter 16.

[8] Wolfgang von Grünhagen, Thorben Schönenberg, Robin Lantzsch, Jeff A. Lusardi, David Lee, and Heiko Fischer. Handling qualities studies into the interaction between active sidestick parameters and helicopter response types. *CEAS Aeronautical Journal*, 5(1):13–28, 2014.

[9] Steffen Greiser, Robin Lantzsch, Jens Wolfram, Johannes Wartmann, Mario Müllhäuser, Thomas Lüken, Hans-Ullrich Döhler, and Niklas Peinecke. Results of the pilot assistance system "assisted low-level flight and landing on unprepared landing sites" obtained with the ACT/FHS research rotorcraft. *Aerospace Science and Technology*, 45:215–227, 2015.

[10] Hyun-Min Kim, Daniel Nonnenmacher, Joachim Götz, Pascal Weber, Edgar von Hinüber, and Stefan Knedlik. Initial flight tests of an automatic slung load control system for the ACT/FHS. *CEAS Aeronautical Journal*, 7(2):209–224, 2016.

[11] Oliver Dieterich, Joachim Götz, Binh Dang Vu, Henk Haverdings, Pierangelo Masarati, Marilena Pavel, Michael Jump, and Massimo Gennaretti. Adverse rotorcraft-pilot coupling: Recent research activities in europe. In *34th European Rotorcraft Forum*, Liverpool, UK, September 2008.

[12] Susanne Seher-Weiß. ACT/FHS system identification including rotor and engine dynamics. In *AHS 73rd Annual Forum*, Fort Worth, TX, May 2017.

[13] Susanne Seher-Weiß. FitlabGui - A versatile tool for data analysis, system identification and helicopter handling qualities analysis. In *42nd European Rotorcraft Forum*, Lille, France, September 2016.